

Concentration gradients in microfluidic 3D matrix cell culture systems

Ioannis K. Zervantonakis¹, Seok Chung², Ryo Sudo³,
Mengwen Zhang⁴, Joseph L. Charest⁵ and Roger D. Kamm^{1,6}

Department of Mechanical Engineering¹, Chemical Engineering⁴ and Biological Engineering⁶, Massachusetts Institute of Technology, Cambridge, MA, USA, Department of Mechanical Engineering², Korea University, Seoul, Korea, Department of System Design Engineering³, Keio University, Yokohama, Japan and Charles Stark Draper Laboratory⁵, Cambridge, MA, USA

Abstract

Microfluidic technology enables the creation of well-defined cell culture environments, which integrate the control of multiple biophysical and biochemical cues for designing novel *in vitro* assays. Growth-factor concentration gradients play a critical role in a wide range of biological processes ranging from development to cancer, guiding cell migration and influencing cell signaling. We present a microfluidic device capable of generating stable concentration gradients in a 3D matrix, while allowing for direct imaging of cellular behavior. The design consists of polydimethylsiloxane microchannels interconnected through 3D matrices. Optical access of the 3D matrix permits direct observation of invasive properties of cells seeded inside the channels or embedded in the matrix. An important characteristic of the microfluidic platform is the capability to generate reproducible, stable and quantifiable concentration gradients that are essential for systematic studies of soluble factor signaling in chemotaxis assays. To characterize the concentration gradients in the device we combine intensity measurements using fluorescent markers and a finite element model, while we also measure the hydraulic permeability and diffusion coefficient of a 40 kDa chemoattractant across the 3D matrix. The numerical model solves the coupled convection-diffusion-Brinkmann equations using a commercial finite element solver. Comparison of measured and computed concentration profiles demonstrates very good agreement, while the simulation can be used as a tool for optimizing the microfluidic design. To demonstrate the device capabilities and the effects of concentration gradients on cell migration, we seeded a brain cancer cell line (U87MG) on the microfluidic channels and monitored cell invasion in 3D type I collagen matrices under control and epidermal growth factor (EGF) gradient conditions. We find that in the presence of an EGF concentration gradient tumor cells are guided towards higher EGF levels and that the directional bias is dependent on the gradient magnitude and EGF concentration. This assay provides new data describing cancer cell invasion in a 3D matrix under control of EGF concentration gradients.

1. INTRODUCTION

Growth-factor concentration gradients play a critical role in a wide range of biological processes from development to cancer, guiding cell migration and influencing cell signaling [1-3]. Motile cells integrate the spatial and temporal characteristics of these chemical gradients to migrate, and may exhibit different migratory characteristics, depending on the gradient steepness. For example, neutrophils and *Dictyostelium amoebae* are able to sense shallow gradients of only a few percent change in chemoattractant concentration across their length [4]. Moreover, chemotaxis is a highly dynamic process with cells responding to a change in the direction of the gradient. Hence, chemotactic

assays need to allow for direct imaging of cells, while enabling the establishment of stable, repeatable and quantifiable gradients for elucidating the effects of different concentration fields on chemotaxis.

Traditional assays in the field such as Boyden chamber, Dunn Chamber and the micropipette radial gradient assay lack precise control of the concentration gradients, are limited in two-dimensional (2D) environments and are not ideal for extracting quantitative cell migration metrics [5]. Microfluidic technology enables the design of novel biological assays to deliver stable concentration gradients, while enabling direct imaging of cell response. Keenan et al provide a comprehensive review describing the latest developments on microfluidic gradient generators, utilizing microvalves, microinjectors, diffusion-based serpentine channels and perfusion-based systems, on a wide variety of cell types including neutrophils, endothelial and cancer cells [5]. Although these designs offer great flexibility in controlling the concentration profile, they are limited to generate gradients on a 2D stiff substrate. Many cell types behave very differently in 2D vs. 3D environments, where cell-extracellular matrix (ECM) adhesion is of critical importance [6]. Furthermore, cells may experience different concentration fields in a 3D environment, since the local concentration field will be influenced by the dimensionality of the experiments and also due to soluble factor-matrix interactions, such as binding and/or release upon proteolytic cleavage. In order to produce more physiologically relevant assays, our group [7-9] and others [10] have presented microfluidic systems incorporating 3D matrices for studies of cancer-fibroblast interactions [11], and dendritic cell migration [12]. However, generating stable and predictable gradients is challenging, due to the inherent coupling of convection and diffusion across a porous 3D matrix. Thus, existing systems [7-9] may be influenced by small perturbations (e.g. pressure differentials) or require gradient buffers which block access to the cells and matrix [12].

In this study we describe a perfusion-based microfluidic platform for generating long-term, stable and quantifiable gradients across a 3D matrix. We characterize experimentally and numerically the convective-diffusive growth-factor fields in this device and compare it with a static three-channel microfluidic system previously developed in our lab which employed only diffusive transport. The diffusion coefficient of a 40 kDa chemoattractant through the collagen type I matrix, and the matrix hydraulic permeability were also measured and compared to previous published data. Through a series of simulations and modeling we predict the effects of the flow-rate in the microchannels on the concentration profiles across the matrix. Finally, we present a 3D chemotaxis assay of brain cancer cells under varying concentrations of epidermal growth factor (EGF) and demonstrate the capabilities of this system in the study of cancer cell invasion.

2. MATERIALS AND METHODS

2.1 Three-channel static culture device

For establishing concentration gradients using solely diffusive effects we employ a static three-channel device [7]. The microfluidic device consists of three independently addressable microfluidic channels, interconnected through porous 3D matrices across which concentration gradients can be established. For pressure equilibration across the 3D matrices and in order to minimize evaporation effects we integrated a second PDMS layer including well reservoirs to supply the diffusible factors (Fig 1(a)). The microfluidic channel dimensions are 120 μm height by 1000 μm width, and the 3D matrix consists of collagen type I at a concentration of 2mg/ml and a polymerization pH 7.4. A more detailed description of the device design, fabrication and experimental procedures can be found in [7].

2.2 Perfusion culture device

The perfusion culture “Y-device” is based on a previous design from our lab for angiogenesis assays [8, 9]. It consists of two microfluidic channels (240 μm height, 500 μm width), interconnected through a matrix region, which then merge further downstream at a Y-junction (figure 1(b)). The system includes a “gel-cage” located between the two parallel channels, upstream of the Y-junction. The gel cage includes a grid of rectangular pillars which add mechanical stability to and constrain the collagen gel 3D matrix by surface tension during microinjection of the matrix in liquid form. The significant system modification presented here is the merging of the two channels for equilibrating the pressures,

in order to minimize flow across the matrix that can perturb the concentration profiles. The flow along the channels required for establishing a gradient across the matrix can be established by an external pump, a pressure source or hydrostatic pressure heads. Here we use a syringe pump (Harvard Apparatus, MA) and an upstream reservoir system, which ensure delivery of equal pressure heads at the inlets. For additional information on the original design and results with angiogenesis assays see [8, 9].

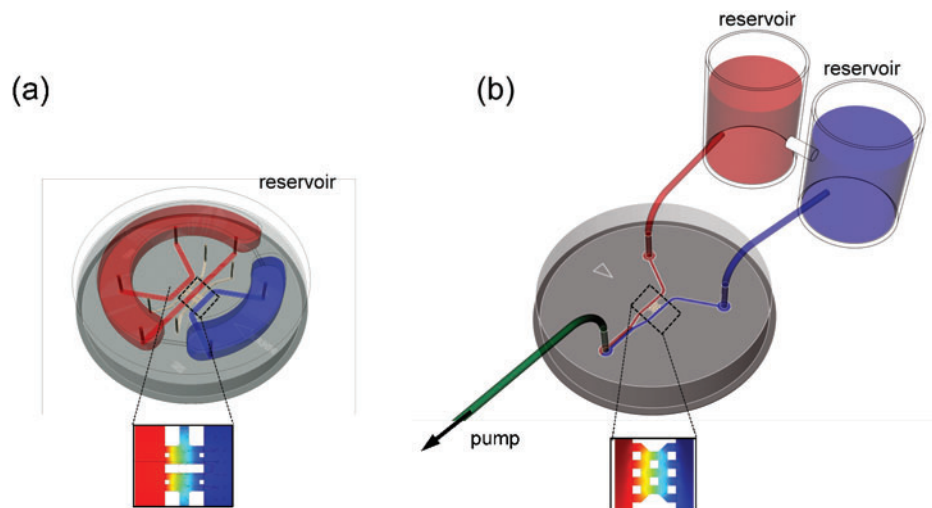


Figure 1. Static three-channel (a) and perfusion (b) microfluidic devices incorporating 3D matrices across which concentration gradients can be established (see inserts)

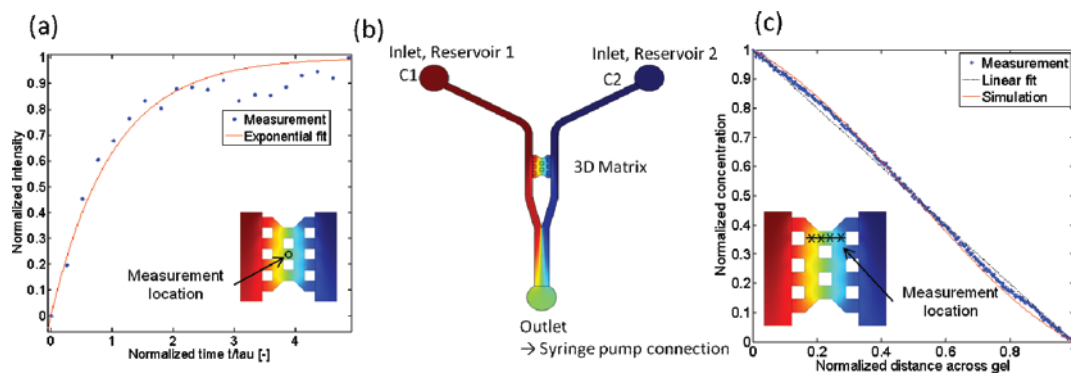


Figure 2. Measurement of 3D matrix (gel) diffusion coefficient by fitting an exponential to the evolution of the fluorescent tracer intensity (a), model geometry and boundary conditions for simulation of the Y-device (b), comparison of measured concentration profiles (blue dotted line) with simulation (continuous red line) and linear profile (black dashed line) at steady state. Inserts outline measurement locations.

2.3 Experimental characterization of concentration fields

Concentration gradients inside the collagen matrix are quantified by combining experimental data and a computational model. Experiments were performed using Texas Red conjugated dextran (Invitrogen, CA) with a molecular weight of 40 kDa, which mimics cytokine (e.g. vascular endothelial growth factor) diffusion in the matrix. The fluorescent conjugated dextran was mixed with phosphate buffered

solution (PBS) (Lonza, MD) to a final concentration of 12.5 $\mu\text{g/ml}$. For the static three-channel system, the fluorescent solution was added to the condition channel, while a tracer-free PBS solution was fed to the other channels, and the fluorescence intensity profiles were recorded every hour using a fluorescent microscope (Nikon, Tokyo, Japan). Similarly, for the Y-device the fluorescent solution was added to one reservoir, while tracer-free solution was added to the other reservoir, and a 6 $\mu\text{l/min}$ flow-rate was applied to perfuse the channels with the solutions. The fluorescence intensity is mapped to a concentration profile by subtracting the background level and normalizing to the initial intensity value at the high concentration channel. The temporal evolution of the intensity profiles is analyzed using Matlab (MathWorks, Natick, MA).

2.4 Measurement of collagen matrix diffusion coefficient and hydraulic permeability

In order to measure the diffusion coefficient we compute the temporal evolution of the fluorescent tracer intensity in a prescribed location within the gel (Figure 2(a)) and fit it to the analytical solution of one-dimensional (1D) diffusion. The first mode ($n = 1$) of the concentration profile under constant source (C_{SOURCE} , $x = L$) and sink (C_{SINK} , $x = 0$) conditions, is given by [13]:

$$C(x,t) = C_{SINK} + \left(C_{SOURCE} - C_{SINK}\right) \frac{x}{L} - \left(C_{SOURCE} + C_{SINK}\right) \frac{\sin(\pi x / L)}{2} \cdot e^{-t/\tau} \quad (1)$$

where x is the space and t are the time variables, L is the matrix width and $\tau = L^2/\pi^2 \cdot D_{Gel}$ is the characteristic time-constant. Using the Matlab curve fitting toolbox we fit a first order exponential to the measured fluorescence intensity time profile within the midpoint of the gel ($x/L = 0.5$) (see Fig 2). We determine a characteristic time $\tau = 54.5$ min, corresponding to a diffusion coefficient of $D_{Gel} = 4.9 \cdot 10^{-11}$ m^2/s for $L = 1250$ μm . This value agrees with the reported values of Helm et al for 2 mg/ml collagen gels [14]. Using equation (1) we can estimate a time that the concentration gradient will have reached 90% of its steady value (see figure 2a) $t/\tau = 2.4$, $t = 2$ hrs.

Pressure differentials across the collagen matrix will give rise to an interstitial flow that can be estimated using Darcy's law:

$$u = K \frac{\Delta P}{\mu \cdot L} \quad (2)$$

where ΔP [Pa] is the pressure drop across the gel, L [m] is the width of the matrix, μ is the fluid dynamic viscosity [Pa·s] and K [m^2] is the hydraulic permeability of the collagen matrix. The value of K can be estimated by recording the pressure drop and the flow-rate across the gel and using equation (2) as outlined in [8]. We measure a value of $K = 10^{-13}$ m^2 , which agrees with values reported by Swartz et al [15] for collagen gels within the same concentration range.

2.5 Computational modeling of concentration profiles

We developed a computational model, combined with the experimental characterization in section 2.3 for systematically investigating growth-factor transport in the microfluidic devices. The model utilizes the coupled transient convection-diffusion and Brinkmann equations, which were solved using a commercial finite element solver in COMSOL (Burlington, MA). The diffusion constant of a 40 kDa inert molecule in the collagen matrix and the matrix hydraulic permeability were based on the measurements described previously, while the diffusion coefficient in the medium was set to $D_M = 6 \cdot 10^{-11}$ m^2/s using the Stokes-Einstein equation. The simulated concentration profiles in the static device have been reported previously [16]. In the Y-device, we defined constant source and sink conditions, a flow-velocity of $u = 10$ $\mu\text{m/s}$, to model the delivery of fluorescent and tracer-free solutions from the reservoirs. At the outlet we defined a zero relative pressure flow condition and a pure-convective outflux $N = u \cdot C$ per unit area, since at the flow velocities studied here, the Peclet (Pe) number is about 100, so convection dominates over diffusion. The computational grid consisted of 400,000 elements. The model boundary conditions, geometry and steady-state solution of the chemo-attractant concentration profiles are shown in Figure 2(b).

2.6 Cancer cell chemotaxis assays

To demonstrate the effects of concentration gradients on cell phenotype we use the U87MG glioblastoma cell line to study cancer cell chemotaxis in the static three-channel devices. U87MG cells were selected because they exhibit single cell migration characteristics through the 3D collagen gel. All cultures were passaged in standard DMEM media supplemented with 10% fetal bovine serum and cultured in a humidified incubator at 5% CO₂ and 37 °C, while the cell passage number was kept lower than 8. A cell suspension at a density of 2·10⁶ cells/ml was introduced into the central microfluidic channel and allowed twenty-four hours for cell attachment. Gradients of EGF were established after the cells had attached on the channels and phase-contrast images of the cell invasion into the collagen gel were acquired every twenty-four hours for three days. Two sets of concentrations, 20 and 200 ng/ml EGF were used for modeling low and high gradients, at two different matrix densities, 2 and 2.5 mg/ml collagen type I gels. As a measure of tumor guidance to the EGF source we quantified cell invasion by measuring the distance migrated in 24 h of the ten fastest cells in the matrix, then computed the difference between cells in the EGF gradient and in the control matrix. Furthermore, the cell migration speed was calculated by the same method mentioned above. The values reported in microns are averages over four independent experiments.

3. RESULTS AND DISCUSSION

3.1 Effects of convection on concentration fields within the 3D matrix

Prior to performing a parameter analysis on the concentration fields using the simulation model, we validated the model by comparing the steady-state concentration profiles within the collagen matrix to experimental measurements. Figure 2(c) shows an excellent agreement between simulation and experiments, and both profiles are approximately linear (dashed black line), as expected at steady-state for 1D diffusion-dominated transport across a homogeneous matrix.

A series of simulations was performed to investigate the effects of varying the flow-rate along the microchannels on the concentration profiles across the collagen matrix (figure 3(a)). At low flow-rates for which convective effects are comparable to diffusion, the concentration distribution along the channel is no longer maintained constant, yielding variable gradients. The dimensionless number defining the relative importance of convection to diffusion is the Peclet (Pe) number:

$$Pe = \frac{u \cdot h}{D} \quad (3)$$

with u [m/s] a characteristic velocity, h [m] a characteristic length-scale and D [m²/s] the diffusion coefficient. Here the characteristic velocity is $u = Q/A$ ($A = 240 \times 500 \mu\text{m}^2$ channel cross-sectional area) with $h = 500 \mu\text{m}$ the channel width, giving a $Pe = 1$ for $Q = 0.04 \mu\text{l/h}$. By increasing the channel flow one ($Pe = 10$) or two ($Pe = 100$) orders of magnitude the concentration along the channel remains constant (figure 3(a)), yielding a constant concentration gradient across the collagen matrix.

A significant challenge for establishing stable concentration profiles within microfluidic systems with integrated porous matrices is to eliminate any interstitial flow across the matrix resulting from pressure imbalances (figure 3(b)). In the three-channel device design where the microfluidic channels are independently addressable, pressure differentials may equilibrate across the porous matrices, resulting in an interstitial flow and disturbances in concentration profile (red dashed line figure 3(b)). For example at a pressure imbalance of 10 Pa, which can be created by a misbalance of 1 mm water pressure-head at the reservoir side, the interstitial flow velocity is estimated at 10 $\mu\text{m/s}$ (equation (2)), or a Peclet number of 10. The concentration profiles for a Peclet number of 10 deviates significantly from the linear diffusion-dominated transport. To overcome this problem, the channels need to be connected either using an external reservoir system (Figure 1(a)) or by including a Y-junction downstream of the “gel cage” region (figure 3(c)). Figure 3(b) shows the concentration profiles across the gel matrix for the Y-device (blue line), which remain nearly linear, contrary to the three-channel device where the concentration profile is disturbed (dashed red line). This can be illustrated by comparing the ratio of the hydraulic resistance R_{Ch} across the channels with the resistance R_{Gel} across

the gel:

$$\frac{R_{Ch}^*}{R_{Gel}^*} = \frac{\mu \cdot L_{Ch}}{A_{Ch} \cdot h_{Ch}^2} \bigg/ \frac{\mu \cdot L}{K \cdot A_{Gel}} \quad (4)$$

where h_{Ch} is the channel height, L_{Ch} is the distance between gel region and point of equal pressure, A_{Ch} and A_{Gel} are the channel and gel cross-sectional areas respectively. This ratio is 1 / 240 000, demonstrating that collagen matrix poses a significant hydraulic barrier normal to the flow, compared to the microfluidic channels.

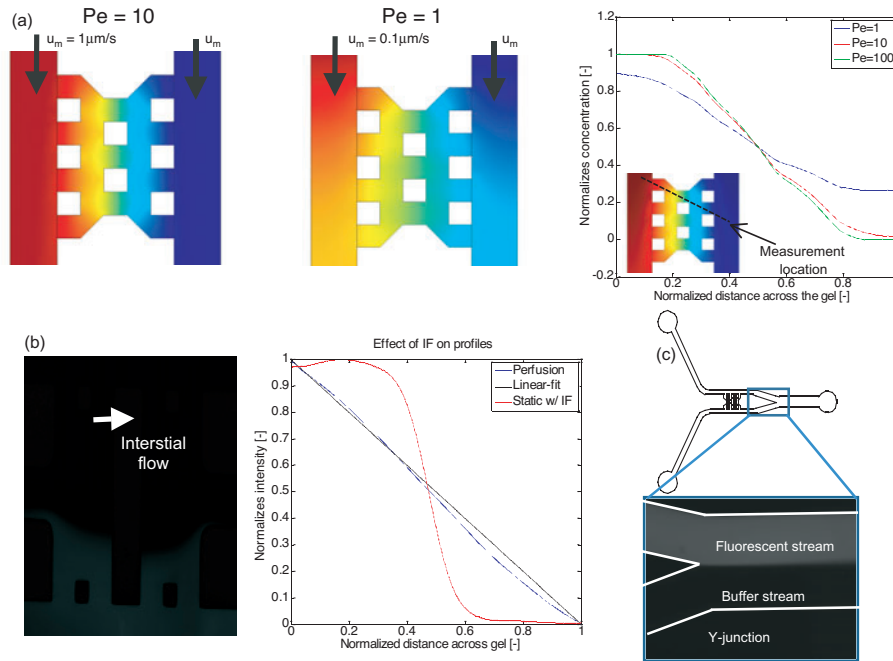


Figure 3. Effects of varying flow-rate in the microfluidic channels on concentration fields across the gel for $Pe=1$ and $Pe=10$. Top right figure shows concentration profiles across the gel (a) Pressure imbalances across the gel result in gradient disturbance for the three-channel device, as shown in the concentration profile (red dashed line), while the Y-device ensures controllable linear gradients (blue line) (b). Fluorescent tracer demonstrates equilibration of pressures across the two channels (c).

Finally, apart from offering valuable quantitative information for our cell migration assays, the developed computational model in combination with experimental data may also be used for optimizing the microfluidic platform for a desired concentration distribution.

3.2 Concentration gradient stability: static versus perfusion system

A significant advantage of the perfusion-based system is its ability to establish a stable and predictable concentration profile. Figure 4 demonstrates the evolution of the measured fluorescent tracer concentration across the matrix for the static (Figure 4(a)) and the perfusion (Figure 4(b)) cases. The slope of the concentration profile (normalized to its initial value) is plotted in the bottom panels of Figure 4, demonstrating that the concentration gradient is diminishing with time in the static three-channel system, while the slope remains nearly constant in the perfusion system. More specifically, a 35% decrease is observed after 12 h. However, this is a low estimate, since uptake by the cells and

binding to the matrix can result to additional depletion, shifting the concentration profiles.

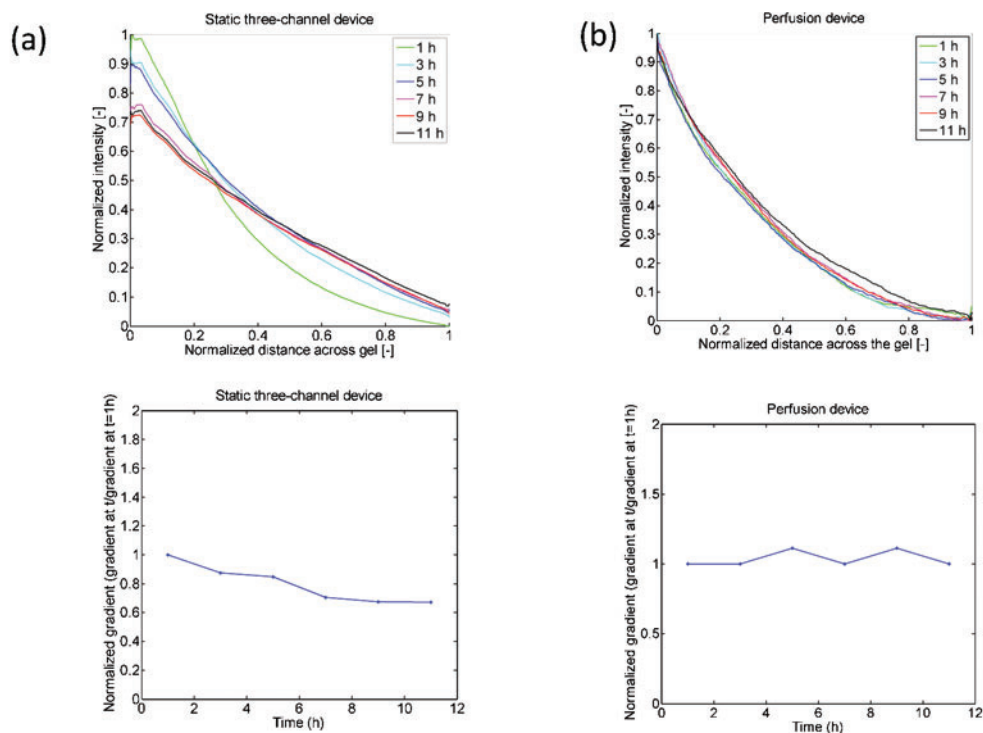


Figure 4. Top row: Evolution of measured concentration profiles across collagen gel in the static three-channel (a) and perfusion device (b). Bottom row: Comparison of normalized gradient stability.

The establishment of stable, quantifiable and reproducible gradients within microfluidic cell culture systems is an important requirement for designing robust biological assays. In our microfluidic systems, 3D collagen matrices are located between microchannels, allowing for gradient establishment by controlling the growth-factor concentration at the matrix boundaries. A minimum channel flow-rate ($Q = 4 \mu\text{l/h}$, $Pe > 10$) is required to eliminate depletion effects in the fluid stream and maintain constant boundary conditions across the matrix. Apart from providing stable gradients, this channel flow may be utilized for applying shear stress on adherent cells cultured on the microchannels. It should be noted that at this low flow-rate, the shear stress applied to cells along the channels is on the order of millipascals. The flow-rate may be increased by a factor of 100 or more to achieve physiological shear stress of 1 Pa (e.g. for endothelial cells), that may induce phenotypic changes to the cells [17].

3.3 Cancer cell chemotaxis in 3D matrices under EGF gradients

We perform a 3D chemotaxis assay to demonstrate the capabilities of our microfluidic platform for establishing chemoattractant gradients and to investigate the effect of gradient magnitude on cancer cell invasion. Brain cancer (U87MG) cells migrate in both the control and gradient collagen matrices. However, quantification reveals a biased invasion, distance that cancer cells moved into the 3D matrix, towards the EGF source as shown in Figure 5 (b) (dashed green arrows). Interestingly, higher matrix density (0.25 % or 2.5 mg/ml) increases the migration bias, likely due to a denser network into which cancer cells can invade into [18]. Furthermore, the tumor cells display less chemotaxis in the 200 ng/ml/1.3mm gradient than in the 20 ng/ml/1.3mm gradient, which may be explained by receptor saturation at higher concentrations [19]. These results also demonstrate an important feature of the

three-channel system for chemotaxis assays: the capability of including both control and test conditions within the same experiment. We also quantify the migration velocity of the cancer cells, and find that the cell migration speed is comparable under the gradient and gradient-free condition for both EGF gradient conditions. However, migration velocity depends on matrix density, as the denser collagen matrix (2.5 mg/ml) results in a migration velocity of 200 $\mu\text{m}/\text{day}$, a two-fold decrease compared with the 2 mg/ml (0.2 %) collagen matrix. The migration velocities measured here agree with values reported for proteolytic invasion [1], where the cells degrade the matrix in order to migrate.

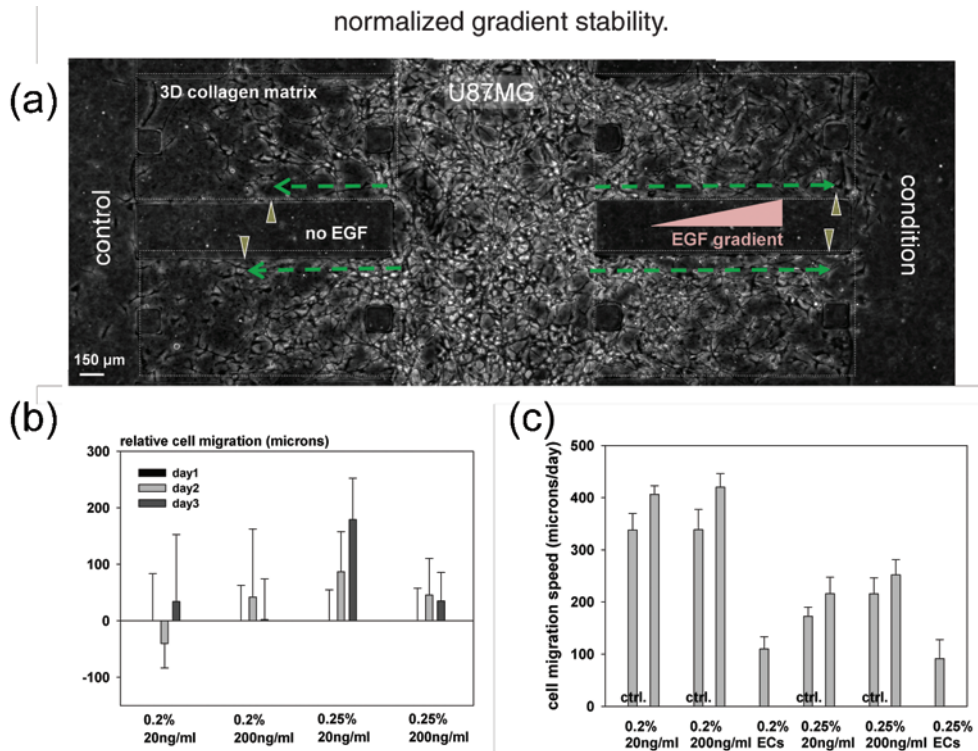


Figure 5. Effect of EGF gradient and collagen gel density on U87MG invasion. (a) Phase-contrast image of tumor cells invading into 3D collagen gel under EGF gradient (right) and control (left) conditions. Direction of invasion is highlighted with the green arrows (b) Quantification of biased migration at different gel densities (0.2% and 0.25%) and concentration gradients (20ng/ml and 200ng/ml). (c) Quantification of cell migration speed for above conditions and under no EGF (ECs) in the control (ctrl.) and gradient matrices.

A significant factor that needs to be considered when designing and interpreting chemotaxis assays is the interplay of the cells with the externally supplied concentration fields and biophysical forces such as interstitial flow and shear stress. Cells may bind and secrete growth-factors as a function of the established gradient and the magnitude of the applied shear stress. This intrinsic coupling can result in deviations from the intended and initially characterized concentration fields. A further complication is that this coupling effect may be flow- or concentration-level-dependent, so that stimulation of the cells with an interstitial flow can affect the rate or amount of factors secreted. To this extent, the growth-factor transport analysis presented here is relevant to chemically inert molecules that do not involve binding to the matrix or to the cells. For addressing this issue, the perfusion Y-device offers a robust platform to maintain well-defined concentration fields, where fluorescently labeled growth-factors may be used for tracking their uptake by the cells and their binding to the matrix.

4. CONCLUSION

In this work, we present a modified system based on our previous designs for achieving long-term, stable, quantifiable concentration gradients across a 3D matrix. By comparing this design with a static three-channel device we demonstrate stable gradients due to the application of a steady channel flow. This channel flow also provides a mechanism to apply controlled, flow-induced shear stress effects on cell migration. We measure the diffusion coefficient and hydraulic permeability of the matrix and develop a numerical model for device design optimization and biological assay design. Finally, we demonstrate that EGF gradients regulate brain cancer cell migration in 3D, resulting in a biased invasion of the cells towards higher EGF concentrations, which is dependent on the gradient magnitude and 3D matrix density.

ACKNOWLEDGEMENTS

This work is supported by The Charles Stark Draper Laboratory University Research and Development Program, NSF-EFRI-0735997 grant and SMART. The authors wish to thank S. de Valence, J. Herrera and P. Bransford for useful discussions on this work. We would also like to acknowledge Dr. HD Kim and Prof. D. Lauffenburger and Prof. F. Gertler for providing us with the brain cancer cell line.

NOMENCLATURE

Symbol	Variable	Units
Q	Flow-rate	[m ³ /s]
ΔP	Pressure differential	[Pa]
μ	Dynamic viscosity	[Pa·s]
K	Hydraulic permeability	[m ²]
u	Flow velocity	[m/s]
A _{Ch}	Microfluidic channel cross-sectional area	[m ²]
A _{Gel}	3D collagen matrix cross-sectional area (normal to flow)	[m ²]
R _{Ch}	Hydraulic resistance of microfluidic channels	[Pa·s/ m ⁴]
R _{Gel}	Hydraulic resistance of collagen gel matrix	[Pa·s/ m ⁴]
C	Concentration	[μ g/m ³]
τ	Characteristic diffusion time	[s]
L _{Ch}	Distance between gel region and point of equal pressure at Y-junction	[m]
L	3D Collagen matrix width	[m]

REFERENCES

1. Friedl, P. and K. Wolf, *Tumour-cell invasion and migration: diversity and escape mechanisms*. Nat Rev Cancer, 2003. **3**(5): p. 362-74.
2. Griffith, L.G. and M.A. Swartz, *Capturing complex 3D tissue physiology in vitro*. Nat Rev Mol Cell Biol, 2006. **7**(3): p. 211-24.
3. Lauffenburger, D.A. and A.F. Horwitz, *Cell migration: a physically integrated molecular process*. Cell, 1996. **84**(3): p. 359-69.
4. Kay, R.R., et al., *Changing directions in the study of chemotaxis*. Nat Rev Mol Cell Biol, 2008. **9**(6): p. 455-63.
5. Keenan, T.M. and A. Folch, *Biomolecular gradients in cell culture systems*. Lab Chip, 2008. **8**(1): p. 34-57.
6. Cukierman, E., et al., *Taking cell-matrix adhesions to the third dimension*. Science, 2001. **294**(5547): p. 1708-12.
7. Chung, S., et al., *Cell migration into scaffolds under co-culture conditions in a microfluidic platform*. Lab on a Chip, 2009. **9**(2): p. 269-275.
8. Sudo, R., et al., *Transport-mediated angiogenesis in 3D epithelial coculture*. FASEB J, 2009. **23**(7): p. 2155-64.

9. Vickerman, V., et al., *Design, fabrication and implementation of a novel multi-parameter control microfluidic platform for three-dimensional cell culture and real-time imaging*. Lab Chip, 2008. **8**: p. 1468-1477.
10. Saadi, W., et al., Generation of stable concentration gradients in 2D and 3D environments using a microfluidic ladder chamber. *Biomed Microdevices*, 2007. **9**(5): p. 627-35.
11. Huang, C.P., et al., *Engineering microscale cellular niches for three-dimensional multicellular co-cultures*. Lab Chip, 2009. **9**(12): p. 1740-8.
12. Haessler, U., et al., *An agarose-based microfluidic platform with a gradient buffer for 3D chemotaxis studies*. Biomed Microdevices, 2009. **11**(4): p. 827-35.
13. Crank, J., *The Mathematics of Diffusion*. 2nd ed. 1980: Oxford University Press. 424.
14. Helm, C.L.E., et al., *Synergy between interstitial flow and VEGF directs capillary morphogenesis in vitro through a gradient amplification mechanism*. Proceedings of the National Academy of Sciences, 2005. **102**(44): p. 15779-15784.
15. Swartz, M.A. and M.E. Fleury, *Interstitial flow and its effects in soft tissues*. Annu Rev Biomed Eng, 2007. **9**: p. 229-56.
16. Chung, S., Sudo, R., Zervantonakis, I.K., Rimchala, T., Kamm R.D. , *Surface-Treatment-Induced Three-Dimensional Capillary Morphogenesis in a Microfluidic Platform*. Advanced Materials, 2009, <http://www3.interscience.wiley.com/journal/122580152/abstract>, DOI: 10.1002/adma.200901727
17. Sill, H.W., et al., *Shear stress increases hydraulic conductivity of cultured endothelial monolayers*. Am J Physiol, 1995. **268**(2 Pt 2): p. H535-43.
18. Yamamura, N., et al., *Effects of the mechanical properties of collagen gel on the in vitro formation of microvessel networks by endothelial cells*. Tissue Eng, 2007. **13**(7): p. 1443-53.
19. Wang, S.J., et al., *Differential effects of EGF gradient profiles on MDA-MB-231 breast cancer cell chemotaxis*. Exp Cell Res, 2004. **300**(1): p. 180-9.